5528–5540 *Nucleic Acids Research, 2006, Vol. 34, No. 19* *Published online 5 October 2006*
doi:10.1093/nar/gkl584

Different modes and potencies of translational repression by sequence-specific RNA–protein interaction at the 5′-UTR

Minghua Nie[1,2] and Han Htun[1,2,*]

[1]Department of Obstetrics and Gynecology and [2]Department of Molecular and Medical Pharmacology, Molecular Biology Institute, University of California Los Angeles-Jonsson Comprehensive Cancer Center, 22-168 CHS, David Geffen School of Medicine at UCLA, 10833 Le Conte Avenue, Box 951740, Los Angeles, CA 90095-1740, USA

Received June 16, 2006; Revised July 24, 2006; Accepted July 25, 2006

ABSTRACT

To determine whether sequence-specific RNA–protein interaction at the 5′-untranslated region (5′-UTR) can potently repress translation in mammalian cells, a bicistronic translational repression assay was developed to permit direct assessment of RNA–protein interaction and translational repression in transiently transfected living mammalian cells. Changes in cap-dependent yellow fluorescent protein (YFP) and internal ribosome entry sequence (IRES)-dependent cyan fluorescent protein (CFP) translation were monitored by fluorescence microscopy. Selective repression of YFP or coordinate repression of both YFP and CFP translation occurred, indicating two distinct modes by which RNA-binding proteins repress translation through the 5′-UTR. Interestingly, a single-stranded RNA-binding protein from *Bacillus subtilis*, tryptophan RNA-binding attenuation protein (TRAP), showed potent translational repression, dependent on the level of TRAP expression and position of its cognate binding site within the bicistronic reporter transcript. As the first of its class to be examined in mammalian cells, its potency in repression of translation through the 5′-UTR may be a general feature for this class of single-stranded RNA-binding proteins. Finally, a one-hybrid screen based on translational repression through the 5′-UTR identified linkers supporting full-translational repression as well as a range of partial repression by TRAP within the context of a fusion protein.

INTRODUCTION

RNA–protein interactions play a key role in many fundamental biological processes through their effects on RNA processing, turnover, transport, localization and translation. Both *in vitro* and *in vivo* approaches have been developed to characterize and detect RNA–protein interactions. Generally, the *in vitro* approach permits detailed biochemical characterization of a particular RNA–protein interaction, while *in vivo* screens identify unknown proteins and RNA target sequence of biological relevance. In this regard, a number of molecular genetic and cell-based assays have been described in prokaryotes and eukaryotes, taking advantage of a biological process or interaction, such as bacteriophage lysogeny, bacterial transcriptional anti-termination, transcriptional activation, ribosome frameshifting, translational repression, genetic complementation and *in vivo* crosslinking to identify interacting partners (1–5).

Of the *in vivo* assays, the yeast three-hybrid system has proven most useful in identifying RNA–protein interacting partners (6). Through generation of two hybrid proteins and a hybrid RNA, the interaction of an unknown RNA-binding protein with its cognate site in a hybrid RNA activates transcription of a synthetic gene, altering a phenotype. In contrast to transcriptional activation-based assay, RNA–protein interaction at 5′-untranslated region (5′-UTR) can result in translational repression in bacteria and eukaryotes (7–9). In eukaryotes, binding of proteins to specific sequences in the 5′-UTR can interfere with cap-dependent recruitment or scanning of the small ribosomal subunit and thereby repress cap-dependent translation of the mRNA, as best illustrated by iron regulation of heavy chain ferritin translation (10–14).

Model studies (15–18) have shown that translational repression in eukaryotic cells by sequence-specific RNA-binding proteins interacting with their cognate binding sites in the 5′-UTR is modest, typically about an order of magnitude. Since these previous studies were based on the recognition of a folded RNA secondary structure or a limited stretch of single-stranded RNA in the 5′-UTR by a sequence-specific RNA-binding protein (10,11,15–17,19–22), we wondered whether a sequence-specific single-stranded RNA-binding protein, which interacted over an extended single-stranded region, could efficiently bind and repress translation of a reporter transcript in mammalian cells (23).

*To whom correspondence should be addressed. Tel: +1 310 206 3015; Fax: +1 310 206 3670; Email: hhtun@mednet.ucla.edu

Bacillus subtilis tryptophan RNA-binding attenuation protein (TRAP) regulates the expression of tryptophan biosynthetic genes by both transcriptional attenuation and translational repression mechanisms (9). TRAP is a multi-subunit complex with 11 identical subunits arranged in a donut-like structure (24,25), which requires L-tryptophan as a co-factor to bind its consensus RNA sequence consisting of 11 GAG or UAG trinucleotide repeats separated by two or three variable 'spacer' nucleotides in the leader region of tryptophan biosynthetic genes (26–31). TRAP has a binding constant of 11 μM for L-tryptophan (32) and a dissociation constant of 0.1–8 nM (24,29,31–34) for RNA. Based on the crystal structures of the related *Bacillus stearothermophilus* TRAP showing an extended single-stranded RNA wrapped around the surface of the TRAP donut (35–38), the stoichiometry of binding single-stranded RNA (28,39) is most likely one *B.subtilis* TRAP oligomer to one 55 nt consensus RNA sequence; however, a 2:1 stoichiometry, obtained from biochemical experiments (32,33), cannot totally be discounted. When bound to TRAP, the *trpE* leader RNA adopts an alternative stem–loop structure leading to both transcriptional attenuation and translational repression, the latter due to sequestration of the Shine–Dalgarno sequence into an RNA hairpin structure preventing ribosome binding and translational initiation in *B.subtilis*; alternatively, TRAP can directly bind its cognate binding site which overlaps both the Shine–Dalgarno sequence and translational initiation region and competitively inhibits ribosome binding for *trpG*, *trpP* and *ycbK* genes (9). Depending on the tryptophan biosynthetic operon, translational repression by TRAP varies but can be as potent as 900-fold for the *trpP* gene (40).

To determine whether *B.subtilis* TRAP or other sequence-specific RNA-binding proteins can bind its recognition sequence to potently repress translation in mammalian cells, we developed a microscopy-based bicistronic translational repression assay to assess RNA–protein interaction based on translational repression through the 5′-UTR in living mammalian cells transiently transfected with appropriate effector (RNA-binding protein) and reporter (RNA transcript with cognate RNA-binding site) DNA constructs. A key component is a bicistronic mRNA reporter transcript with two independent sites of translational initiation (41) for two spectrally distinct reporter proteins (42). Examination of a field of 30 transfected cells allows reliable determination for presence of a specific RNA-binding activity. With digital fluorescence microscopy, not only can reporter gene activity be assessed qualitatively but also the magnitude change in reporter gene activity can be quantified from a cell-by-cell measurement of the fluorescent intensity for the two fluorescent reporter proteins.

Using this microscopy-based bicistronic translational repression assay, two modes of translational repression, selective or coordinate, were observed, leading to a range of translational repression from 1.5- to 180-fold for four RNA–protein interactions. Although three of the four RNA-binding proteins showed translational repression of less than one order of magnitude, not atypical for translational repression through the 5′-UTR in eukaryotic cells (10,15–22,43–45), *B.subtilis* TRAP with over two orders of magnitude showed that translational repression by sequence-specific RNA-binding protein through the 5′-UTR can be robust in mammalian cells. Finally, linkers that preserved the RNA-binding activity of a TRAP–green fluorescent protein (GFP) fusion protein were identified through a limited screen of a random linker library in mammalian cells.

MATERIALS AND METHODS

Plasmids

Transcription from a cytomegalovirus (CMV) immediate early enhancer/promoter produces a bicistronic mRNA encoding multiply epitope-tagged yellow fluorescent protein (YFP) and cyan fluorescent protein (CFP), whose translation depends on 5′ cap and internal ribosome entry sequence (IRES), respectively (Figure 1a). To obtain this bicistronic reporter gene, called pYIC DNA, the EGFP sequence in pIRES2-EGFP (Clontech) is replaced between the BstXI and NotI sites with PCR-amplified product of CFP sequence from pECFP-Mito (Clontech) tagged at the C-terminus with one copy of hemagglutinin (HA) and polyhistidine (His_6) (46). CFP translation is dependent on encephalomyocardiatis virus IRES (7,41,47). Similarly, YFP sequence from pEYFP-N1 (Clontech) was PCR amplified to contain FLAG and His_6 epitope sequences in frame at the C-terminus, and this PCR product was inserted between the 5′-UTR and IRES at SacI and EcoRI sites. In addition, oligonucleotides for three c-myc epitope tags (46) were inserted in frame at SacI and BssHII sites to tag the N-terminus of YFP. Unlike the downstream CFP cistron, translation of the upstream YFP cistron is cap-dependent. Presence of multiple epitope tags in CFP and YFP yield proteins with predicted molecular weight of 29.6 kDa (262 amino acids) and 33.3 kDa (293 amino acids), respectively, and result in distinct electrophoretic mobilities.

Oligonucleotides with a 55-nt TRAP-binding sequence, TBS (9), were inserted into pYIC DNA at four different restriction enzyme sites to generate bicistronic reporter genes with TBS at different locations: SacI site for 5′-UTR (pTBS/5Y-YIC; 45 nt downstream of transcription start site and 9 nt upstream of YFP translational start site), BssHII site for YFP coding region (pTBS/iY-YIC; 112 nt downstream of translational start site between c-Myc epitope tags and YFP coding region), BamHI site for 3′-UTR of YFP (pTBS/3Y-YIC; 48 nt downstream of stop codon for YFP and 7 nt upstream of IRES) or NotI site for 3′-UTR of CFP (pTBS/3C-YIC; 48 nt downstream of stop codon for CFP). Similar strategy was used to introduce into the 5′-UTR two copies of bacteriophage MS2 coat protein (MS2-CP) binding sites, 2xMS2 (48,49), at BglII and SacI sites (p2MS2-YIC; 33 nt downstream of transcription start site and 9 nt upstream of YFP translational start site), one copy of H-ferritin iron response element, IRE (10,11,16), at NheI and SacI sites (pIRE-YIC; 15 nt downstream of transcription start site and 9 nt upstream of YFP translational start site) or one copy of mouse vRNA obtained by PCR amplification of vRNA from MVG vector (50) (from Valerie Kickhoefer, UCLA) at BglII and SacI sites (pvRNA-YIC; 33 nt downstream of transcription start site and 9 nt upstream of YFP translation start site). Formation of specific RNA–protein complex within 60 nt of transcription start site should interfere with either recruitment or scanning of the 43S translational preinitiation complex and thereby repress translation (13–15,19). Introduced sequences

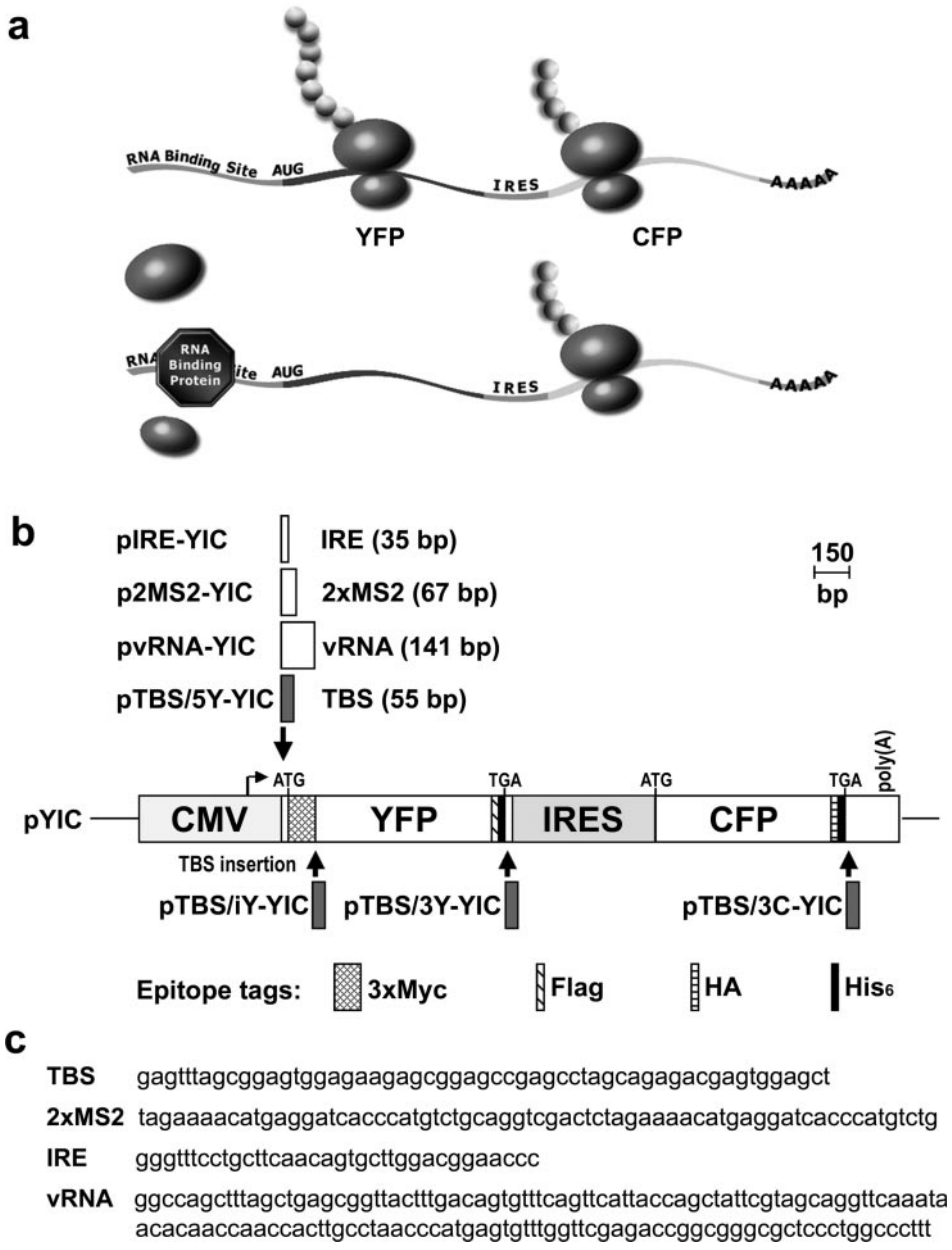

Figure 1. Assessment of RNA–protein interaction through selective translational repression of bicistronic reporter transcripts. (**a**) Schematic diagram illustrating the principle underlying the bicistronic translational repression assay. A bicistronic reporter gene that encodes YFP and CFP on a single mRNA is expressed in a mammalian cell line, such as 293T cells, by transient transfection. A RNA-binding protein recognition site is introduced within the 5′-UTR of YFP. In the absence of RNA-binding protein, both YFP and CFP are expressed. Presence of a sequence-specific RNA-binding protein at its cognate site in the 5′-UTR interferes with the loading or scanning of 40S preinitiation complex and thereby inhibits YFP translation. CFP translation via IRES is not affected and provides a second signal for unambiguously identifying transiently transfected cells as well as an internal control for normalizing cell-to-cell variation in reporter transcript level and capacity for translation. (**b**) Schematic representation of bicistronic reporter gene constructs. Transcription mediated by cytomegalovirus (CMV) enhancer/promoter in the parental pYIC expression DNA yields a bicistronic reporter transcript encoding multiply epitope-tagged YFP and CFP, whose translation is dependent on 5′ cap or IRES, respectively. Single boxed area associated with downward or upward arrow indicates RNA recognition motif and position of insertion in pYIC DNA to yield the bicistronic reporter gene plasmid DNA named on left. Scale bar in bp. (**c**) Sequence of the RNA-binding protein recognition motifs. TBS for TRAP-binding site, 2xMS2 for two MS2-CP-binding sites, IRE for iron response element or vRNA for vault RNA.

in pYIC DNA were confirmed on an ABI 3700 Capillary DNA Analyzer using BigDye Terminator (Applied Biosystems), as per the manufacturer's instructions.

A modified pCI mammalian expression DNA (Promega), pCI-cH6HA-T7term, was used to express *B.subtilis* TRAP and bacteriophage MS2-CP in mammalian cells by inserting PCR product of *mtrB* from *B.subtilis* (ATCC) at NcoI (partial digestion) and EcoRI sites and PCR product of MS2-CP coding sequence (51) from pGEX-MS2 (from Douglas Black, UCLA) at NcoI (partial digestion) and BssHII sites. A strong cytomegalovirus (CMV) enhancer and promoter drive the expression of both wild-type proteins. Both TRAP and MS2-CP are tagged at the C-terminus with HA and His_6 epitopes (46). DNA sequence determination confirmed

the identity of the different DNA constructs. Detailed information on DNA constructs can be provided upon request.

Media and buffers

Supplemented DMEM: (DMEM; Cellgro) with 10% fetal bovine serum (Hyclone), 2 mM L-glutamine, 100 U/ml penicillin and 100 μg/ml streptomycin. Phosphate-buffered saline (PBS) buffer: 137 mM NaCl, 2.7 mM KCl, 10 mM Na_2HPO_4 and 2 mM KH_2PO_4 adjusted to pH 7.4 with HCl. Lysis buffer: 50 mM Tris, pH 7.5, 100 mM NaCl, 5 mM EDTA, 1% Triton X-100 and EDTA-free Complete Mini Protease Inhibitor cocktail (Roche). Western blot blocking buffer: 5% nonfat dry milk in PBS with 0.1% Tween-20. Supplemented NCI buffer: 20 mM HEPES, pH 7.8, 140 mM NaCl, 1.5 mM $MgCl_2$ supplemented with 250 U/ml SUPERase-In (Ambion), 0.5% NP-40 and 1 mM DTT.

Cell transfections

The 293T, MEF 11 (*mTep1*$^{+/+}$) and MEF 8 (*mTep1*$^{-/-}$) cells grown overnight in supplemented DMEM in a humidified 5% CO_2, 37°C incubator (50,52) were transfected next day by a calcium phosphate method (53) at 70% confluency with 4 μg DNA for 35 mm dish and 8 μg DNA for 60 mm dish using pUC19 as carrier DNA. Media were changed 16 h after transfection with cells returned to 5% CO_2 for additional 8 h recovery before analysis. To activate iron regulatory proteins (IRPs) in 293T cells, 100 μM deferoxamine mesylate (Sigma) was added with the reporter gene (11). For linker screen, transfections were carried out in 293T cells with 2 μg DNA for each well of a 24-well flat bottom plate, and cells recovered for additional 30 h before microscopy.

Fluorescence microscopy

Cellular fluorescence was examined on an Olympus IX-70 microscope with a 100 W mercury arc lamp using a −40°C, 12-bit CCD camera, phase contrast UPlanFl 20×/0.50 NA objective, multi-band beam splitter (Chroma) and excitation/emission filters (436 ± 5 nm/470 ± 15 nm for CFP, 490 ± 10 nm/528 ± 19 nm for GFP, 500 ± 10 nm/535 ± 15 nm for YFP, 555 ± 14 nm/617 ± 36.5 nm for DsRed2). Fluorescence was quantified for a 10-pixel radius in a cell using Data Inspector function of the SoftWoRx software (Applied Precision). Background corrected (mean of 10 measurements in an area with no cells) fluorescence values were used to calculate YFP/CFP fluorescence ratio for each cell and then the mean and SD of YFP/CFP fluorescence ratio from 30 cells. For MS2-CP, the background corrected YFP and CFP fluorescence were used to calculate mean and SD of YFP and CFP fluorescence ($n = 30$). Cells without CFP (untransfected cells) or with saturated pixels (value >4094) were excluded from the quantitative analysis.

Statistical analysis

Coefficient of variation was calculated by dividing SD of a population by its mean. To test statistical significance of differences in the mean and SD, a two-tailed non-parametric, distribution-free Wilcoxon rank sum test (also called Mann–Whitney *U*-test) was performed with an alpha level of 0.05 and $n = 30$ for each sample (54). The null hypothesis is that two populations have identical median values with identical distributions.

Western blot analysis

Cells were rinsed with PBS, pelleted at 16 000 *g* for 10 s, resuspended in lysis buffer, frozen (−70°C), thawed on ice and centrifuged (16 000 *g*, 4 min). Protein concentration of supernatant was determined by Bradford method (55) using Bio-Rad Protein Assay. Extract (50 μg) was separated by 12% polyacrylamide (acrylamide/bisacrylamide 30:1)–0.1% SDS gel and transferred on to nitrocellulose. Membrane was incubated in blocking buffer, probed with rabbit polyclonal anti-His_6 antibody (1:2000) (Affinity BioReagents) and horseradish peroxidase goat anti-rabbit IgG secondary antibody (1:10 000) (Zymed), and developed with Pierce West Pico Substrate (55). Chemiluminescence was captured by X-ray film or 8-bit CCD camera (AlphaInnotech ChemiImager) with data from the latter used to determine total pixel value of a rectangular area with vendor-supplied 2D spot density tool. Background corrected (total pixel value of same size rectangle from region lacking signal) YFP and CFP pixel values were used to calculate YFP/CFP protein ratio.

Northern blot analysis

RNA was isolated with Qiagen RNeasy kit, according to the manufacturer's instructions. For nuclear RNA, freshly pelleted cells were resuspended and lysed on ice for 1 min in supplemented NCI buffer. Lysate was laid on NCI with 1% NP-40 and 24% sucrose, and centrifuged (7500 *g*, 15 min, 4°C). Supernatant was mixed with RLT buffer (Qiagen) and total, cytoplasmic and nuclear RNAs were separated on a 1% agarose gel with 1× MOPS buffer and 6% formaldehyde. Northern blot analysis was performed as described previously (55). After transfer and UV crosslinking, Hybond-N membrane (Amersham) was hybridized to ^{32}P-labeled anti-sense RNA probes (Promega) for bicistronic or glyceraldehyde-3-phosphate dehydrogenase (GAPDH) transcripts. Radioactivity was detected and quantified on a STORM860 PhosphorImager (Molecular Dynamics). Ethidium-stained pre-ribosomal, mature 28S and 18S rRNAs served as loading and fractionation controls.

Linker screen for functional TRAP–GFP fusion protein

To replace YFP coding sequence in the bicistronic gene with TBS in the 5′-UTR, the pTBS/5Y-YIC DNA (Figure 1b) was digested with SpeI and XhoI and YFP coding sequences replaced with SpeI–XhoI digested PCR-amplified DsRed2 coding sequence from pDsRed2-N1 (Clontech) to obtain pTBS/5Y-RIC DNA. To obtain mammalian expression DNAs with different linkers for TRAP–GFP fusion proteins, a previously constructed TRAP–GFP mammalian expression DNA with TRAP fused to the N-terminus of GFP (EGFP; Clontech) through five glycine-alanine repeats (GA5 linker) was used. A unique BssHII site at the end of the GA5 linker permitted insertion of a series of 26- or 56-bp BssHII fragments coding 9 or 19 random amino acids, respectively. The two series of BssHII fragments were obtained by BssHII digestion of a Klenow fill-in reaction (55) after annealing the complementary oligonucleotide (5′-GACTCACCAGCGCGC-3′)

to oligonucleotides 5′-tgacaacatgGCGCGCNY(NNY)$_7$-NGCGCGCtggtgagtc-3′ and 5′-tgacaacatgGCGCGCNY-(NNY)$_{17}$NGCGCGCtggtgagtc-3′. To prevent introduction of a stop codon for one linker orientation, the third position of a codon specified a pyrimidine nucleotide. Plasmid DNAs were isolated from 105 bacterial transformants (25, shorter linker; 80, longer linker) using Plasmid Mini Kit (Qiagen) and quantified with Hoescht dye on a VersaFluor (Bio-Rad) fluorometer.

To assess the RNA-binding of different TRAP–GFP fusion proteins, 8×10^4 293T cells were placed in a well with 1 ml supplemented DMEM for five 24-well flat bottom plates (Falcon). Next day, 2 μg DNA transfection mixture (0.4 μg bicistronic reporter DNA (pTBS/5Y-RIC) and 1.2 μg TRAP-expression DNA, TRAP–GFP expression DNAs or pUC19) in 100 μl volume was applied drop-wise to each well and cells placed in a humidified 3% CO_2-37°C incubator (53). After media change 16 h later, cells were returned to a humidified 5% CO_2-37°C incubator and left to recover for 30 h.

Transfection with the reporter gene alone, reporter gene in the presence of TRAP, and reporter gene with TRAP fused to GFP by a GA5 linker were performed for every plate and served as controls for plate-to-plate variability and image capture conditions. With a phase UPlanFl 20×/0.50 NA objective, exposure times were determined from these controls to permit greatest dynamic range, minimal bleed through, and sensitivity at 0.02 sec for DsRed2 (555 ± 14 nm excitation/617 ± 36.5 nm emission filters), 0.05 s for GFP (490 ± 10 nm excitation/528 ± 19 nm emission filters) and 0.5 s for CFP (436 ± 5 nm excitation/470 ± 15 nm emission filters). Under these exposure conditions, control transfection of 293T cells with pTBS/5Y-RIC DNA alone had saturated pixels for DsRed2 fluorescence (with saturated images shown in Figure 5a) but not for other fluorescence or transfections. For each well, four fields were imaged to ensure presence of transfected cells in the imaged field by automatic, pre-determined stage movements in the *x*–*y* direction, as transfected 293T cells are easily dislodged from the bottom surface of the plate.

Captured images were analyzed as overlays of the three different fluorescence after contrast stretching pixel values over the range 60–1000 for DsRed2 (pseudocolored red), 60–300 for CFP (pseudocolored blue) and 60–2000 for GFP (pseudocolored green). Under these visualization conditions, all three fluorescence are readily evident for TRAP–GFP with GA5 linker. Potential positive linkers were defined as linkers suppressing red fluorescence signal below that of the GA5 linker. To further verify improved RNA-binding ability, Western blot analysis was performed on 293T cells plated in 35 mm dishes and co-transfected with 1 μg pTBS/5Y-YIC DNA and 3 μg TRAP–GFP expression DNA, TRAP-expression DNA or pUC19 DNA, essentially as described above.

RESULTS

Rationale of the bicistronic translational repression assay

To directly assess RNA–protein interaction and translational repression by sequence-specific RNA-binding proteins in transiently transfected living mammalian cells, we took advantage of a well-documented biological phenomenon, namely cap-dependent translational repression by sequence-specific RNA-binding protein through the 5′-UTR (7,10,11, 13–16,19–22,43,56,57). Since transient transfection is highly variable, careful choice of transfection system, optimization of parameters, DNA titrations and multiple repetitions are often required for reliable results. When coupled to an assay such as translational repression, loss or lower reporter gene signal could simply be due to inefficient or no transfection. A bicistronic mRNA with independent sites for ribosome loading should provide a means to positively identify transfected cells and normalize for cellular variations encountered with transient transfection, and thereby allow development of a microscopy-based approach to assess RNA–protein interaction and translational repression.

Figure 1a illustrates the underlying principle of the assay in which a single RNA transcript encodes for two spectrally distinct fluorescent proteins, YFP and CFP (42), whose translational initiations occur at two independent sites: 5′ cap to yield YFP and an encephalomyocardiatis virus IRES to yield CFP (7,41,47). An RNA recognition site is inserted between the 5′ end of the message and the YFP coding sequences. In the simplest scenario, a specific RNA–protein complex in the 5′-UTR should interfere with the loading or scanning of 40S ribosomal preinitiation complex for the cap-dependent pathway, reducing YFP translation (13,14, 19), but not interfere with small ribosomal subunit loading for the cap-independent pathway at the IRES, thereby not affecting CFP translation (41,58,59). YFP and CFP fluorescence can be directly visualized in living cells and their relative fluorescence (YFP/CFP) quantified by digital fluorescence microscopy. With a sequence-specific RNA–protein interaction at the 5′-UTR, a decrease in the YFP/CFP fluorescence ratio is expected.

Four RNA–protein interactions were evaluated using bicistronic reporter genes with RNA-binding motif inserted in the 5′-UTR within 60 nt of the transcription start site and 9 nt upstream of YFP translation initiation codon (Figure 1b, downward arrow and Figure 1c). For human IRPs–IRE interaction (7,10,11,13,14) and mouse telomerase/vault-associated protein (TEP1)–vault RNA (vRNA) interaction (60), only the bicistronic reporter gene was transfected into a human embryonic kidney cell line, 293T (52) or congenic mouse fibroblast cell lines, Tep1$^{+/+}$ and Tep1$^{-/-}$ (50), respectively. For *B.subtilis* TRAP (9) and bacteriophage MS2 coat protein (MS2-CP) (61,62), effector expression DNA and bicistronic reporter gene were co-transfected into 293T cells. Aside from the TEP1–vRNA association which is weak and has not fully been determined (60), the binding affinities for the other three protein–RNA interacting pairs are in the nanomolar to subnanomolar range (18,24,29,31,33).

Direct assessment of RNA–protein interaction through selective translational repression

We examined a well-characterized RNA–protein interaction between IRPs and IRE to test the bicistronic translational repression assay in mammalian cells. In iron-starved cells, IRPs repress H-ferritin translation by binding to a single IRE in the 5′-UTR of H-ferritin mRNA (7,10,11,13,14). The 293T cells, transfected with an IRE-containing bicistronic

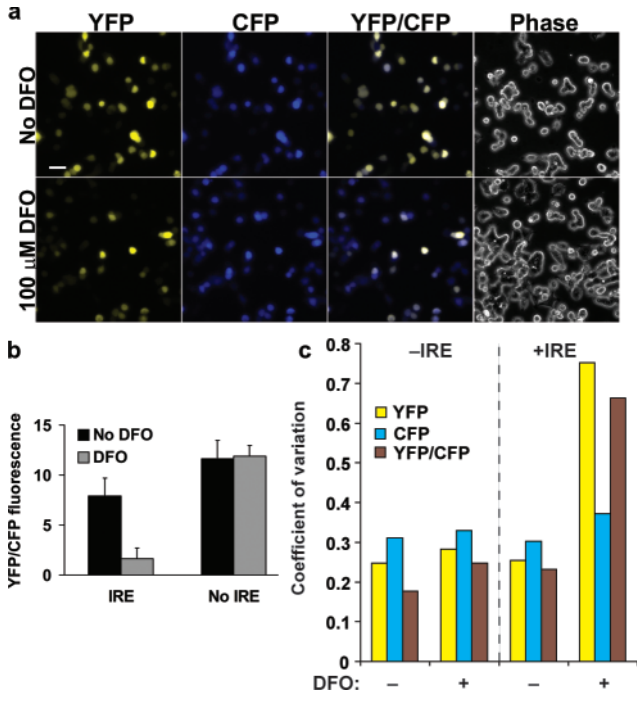

Figure 2. Assessment of IRP–IRE interaction in living mammalian cells after transient transfection of an IRE-containing bicistronic reporter gene. (**a**) Fluorescence and light microscopy images of YFP and CFP production in cells with IRE-containing bicistronic message. Cells were transiently transfected in a 35 mm dish with a bicistronic reporter gene, containing IRE in the 5′-UTR (1 μg pIRE-YIC DNA), and treated at the start of the transfection with no deferoxamine mesylate (No DFO; upper panels) or 100 μM deferoxamine mesylate to activate endogenous IRPs (100 μM DFO; lower panels). YFP and CFP fluorescence are pseudocolored yellow (YFP) and blue (CFP), respectively, and also superimposed (YFP/CFP). Phase contrast image of each field of cells analyzed by fluorescence is shown in the last panel of each row (Phase). Scale bar, 40 μm. (**b**) Quantitative evaluation of YFP and CFP fluorescence microscopy data for differential changes in YFP over CFP level. Mean of the relative YFP fluorescence (YFP/CFP fluorescence) from 30 randomly selected cells within one microscope field is shown for cells transfected with an IRE-containing bicistronic reporter gene (IRE; pIRE-YIC DNA) or no IRE-containing bicistronic reporter gene (No IRE; pYIC DNA) and treated at the start of the transfection with 100 μM deferoxamine (DFO) to activate endogenous IRPs or no deferoxamine (No DFO). Relative YFP fluorescence was calculated by dividing YFP fluorescence by CFP fluorescence for each 10-pixel radius circle placed within a cell after correcting for background fluorescence outside of the cell. Error bars represent SDs. Activation of endogenous IRPs by DFO significantly reduced YFP/CFP fluorescence for IRE-containing bicistronic gene (P-value $= 5.52 \times 10^{-11}$ by Wilcoxon rank sum test) but had no significant effect on IRE-lacking bicistronic gene (P-value $= 0.78$). (**c**) Coefficient of variation for samples plotted in (b) showing the value of normalizing YFP signal by CFP. In the absence of IRP–IRE interaction at the 5′-UTR (−IRE, left-hand side), there was less variation in the normalized YFP signal compared to YFP alone (compare brown and yellow bars within each group). In contrast, a significant rise in YFP/CFP coefficient of variation occurred upon activation of endogenous IRPs in cells with the IRE-containing bicistronic reporter gene (compare right most brown bar with three previous brown bars). +IRE and −IRE refer to IRE and No IRE samples in (b), respectively.

reporter gene, pIRE-YIC, expressed YFP and CFP, evident from yellow and cyan fluorescence (Figure 2a, No DFO). Activation of endogenous IRPs by iron-chelator deferoxamine (DFO) selectively decreased yellow fluorescence (compare No DFO versus 100 μM DFO), with primarily blue instead of yellow-white cells in the YFP/CFP overlay. Note YFP/CFP overlay readily distinguishes cells with repressed

Table 1. Translational repression by RNA-binding proteins interacting at the 5′-UTR

Target site	RNA-binding protein		Fold repression	P-value, Wilcoxon rank sum test
	−	+		
TBS	14.45 ± 2.69	0.08 ± 0.06	180.6	3.04×10^{-11}
IRE	7.89 ± 1.82	1.62 ± 1.08	4.9	5.52×10^{-11}
2xMS2	2.31 ± 0.67	2.53 ± 0.62	0.9	0.20
vRNA	7.36 ± 1.55	4.84 ± 1.46	1.5	5.61×10^{-7}

Mean of YFP/CFP fluorescence and its SD calculated from 30 mouse or human cells transiently transfected with bicistronic reporter gene containing RNA recognition sequence (target site) in the 5′-UTR. In addition, RNA-binding protein status indicates co-transfection status of TRAP-expression DNA for TBS or MS2-CP expression DNA for 2xMS2, activation status of endogenous IRPs by iron-chelator deferoxamine for IRE, and transfection into *mTep1*$^{-/-}$ or *mTep1*$^{+/+}$ cells for vRNA. Fold repression of translation by RNA–protein interaction was calculated by dividing mean YFP/CFP fluorescence value in the absence of the RNA-binding protein by that in its presence. To establish statistical significance in the mean YFP/CFP values given in the second and third columns, Wilcoxon rank sum test was performed with the YFP/CFP fluorescence values ($n = 30$) used to calculate each mean and the result of this test reported as a P-value in the last column.

YFP translation from untransfected or unrepressed cells—not possible with YFP data alone.

Shift from yellow-white to blue color with endogenous IRP activation suggests selective repression of cap- over IRES-dependent translation. Quantification of YFP and CFP fluorescence showed the mean YFP/CFP fluorescence ratio ($n = 30$) to decrease ~5-fold from 7.89 ± 1.82 to 1.62 ± 1.08 with endogenous IRP activation (Figure 2b, IRE; Table 1, P-value $= 5.52 \times 10^{-11}$, all P-values were obtained by Wilcoxon rank sum test (54) on two samples with $n = 30$ for each), consistent with measurements in previous studies (10,16,44). Without an IRE, iron chelation did not alter YFP/CFP ratio (Figure 2b, No IRE; P-value $= 0.78$). Thus, activation of endogenous IRPs selectively represses cap-dependent translation through an IRE in the 5′-UTR of a bicistronic reporter transcript.

Coefficient of variation analysis shows the value of normalizing YFP signal with CFP signal. As shown in Figure 2c for cells lacking IRP–IRE interaction (first three groups), the coefficient of variation for YFP fluorescence is always higher before normalization (yellow bar) than after normalization (brown bar), making YFP/CFP ratio a more reliable measure for studying translational effects when faced with problems of cell-to-cell differences in reporter transcript level and capacity for translation. With IRP–IRE interaction, a significant rise in YFP/CFP coefficient of variation occurs, indicating YFP and CFP levels do not necessarily correlate with each other (compare right most brown bar with three previous brown bars). Thus, IRP–IRE interaction can be directly assessed and quantified from a limited number of transiently transfected living mammalian cells ($n = 30$) using a bicistronic reporter gene with YFP/CFP coefficient of variation as an additional indicator of selective translational repression.

Potent translational repression by TRAP in mammalian cells

To determine if *B.subtilis* TRAP can bind its consensus sequence in the 5′-UTR and repress translation of a reporter transcript in mammalian cells, we examined mammalian

cells transfected with a bicistronic gene (pTBS/5Y-YIC, Figure 1b) containing a 55 nt TRAP-binding sequence, $[(U/G)AGnn]_{11}$ (TBS), which showed strong yellow and modest cyan fluorescence (Figure 3a). Co-transfection with TRAP-expression DNA greatly suppressed yellow fluorescence, with striking differences seen in the YFP/CFP overlay. Quantitative analysis showed dose-dependent decrease in YFP/CFP fluorescence for the reporter gene with TBS in the 5′-UTR (Figure 3b), producing ~180-fold decrease in YFP/CFP fluorescence for TRAP–TBS interaction at 6 μg TRAP-expression DNA (Table 1, P-value $= 3.04 \times 10^{-11}$). YFP/CFP coefficient of variation increased with TRAP–TBS interaction, consistent with selective translational repression by TRAP decreasing the positive correlation in YFP and CFP levels observed in the absence of TRAP–TBS interaction (Figure 3f). Northern blot analyses showed no TRAP effect on the ~2 kb bicistronic mRNA, ruling out mRNA availability or turnover as mechanisms for decreased YFP level (data not shown). Thus, the bicistronic translational repression assay detects very potent translational repression by bacterial TRAP in mammalian cells—illustrating that translational repression by sequence-specific RNA–protein interaction at the 5′-UTR can exceed the one order of magnitude, typically reported in model eukaryotic studies (15–18).

Validation of visualization results

For independent confirmation of the visualization analyses, western blot analyses were performed on extracts prepared from the same pool of cells examined in Figure 3b. Anti-His_6 antibody detected three bands at the expected molecular weight for His_6-tagged YFP, CFP and TRAP (~33, 30 and 12 kDa, respectively; Figure 3c). Without TRAP, YFP is expressed at a higher level than CFP (lanes 1 and 6). TRAP expression reduced YFP expression in a dose-dependent manner for the TBS-containing bicistronic gene (lanes 2–5) but not one lacking TBS (lane 7). At the highest TRAP level (lane 5), YFP repression was ~141-fold, quantified using a CCD camera-based system for chemiluminescence detection (AlphaInnotech ChemiImager). This degree of repression was slightly less than ~180-fold determined by fluorescence microscopy (Figure 3b and Table 1). Thus, western blot and fluorescence microscopy data show a high degree of concordance revealing qualitatively dose- and sequence-dependent repression of cap-dependent translation by TRAP and quantitatively selective translational repression of over two orders of magnitude in strength.

Position dependence of RNA-binding site for translational repression

Potency of TRAP translational repression prompted us to examine if other positions within the RNA can serve to repress translation (Figure 1b, upward arrows). Placement of TBS within the translated region of the epitope-tagged YFP (pTBS/iY-YIC), 3′-UTR of YFP (pTBS/3Y-YIC) or 3′-UTR of CFP (pTBS/3C-YIC) had negligible effect on the relative YFP fluorescence or protein level (Figure 3d and e). Thus, translational repression by TRAP is position-dependent and only effective through interaction at the 5′-UTR (Figure 3a–c).

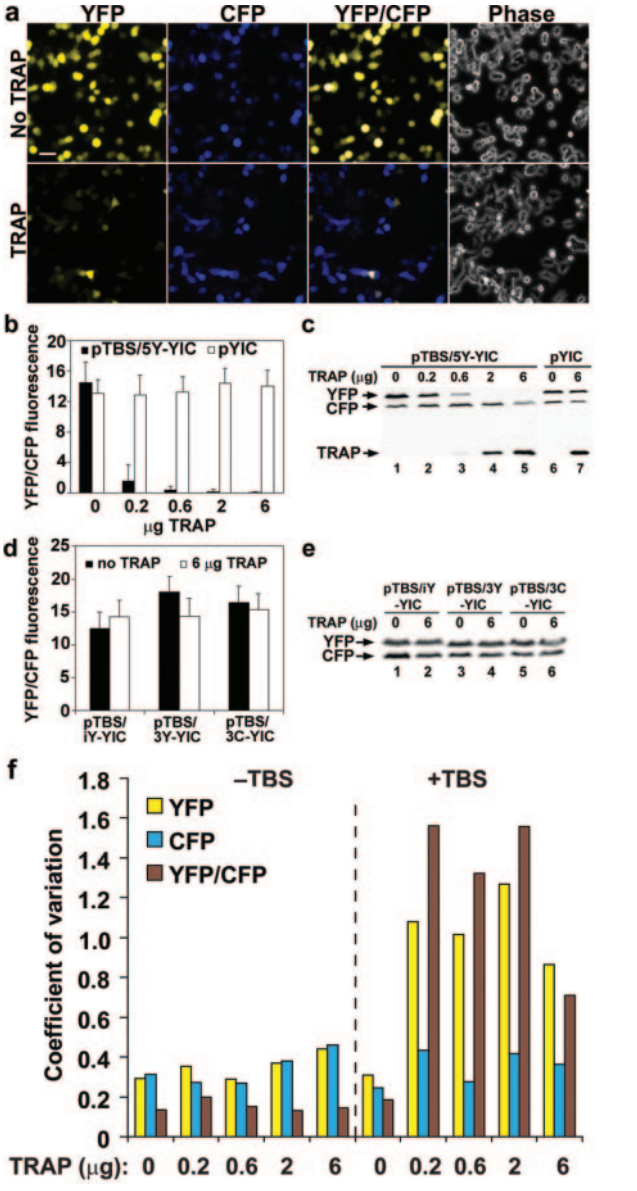

Figure 3. Potent translational repression of YFP expression by TRAP through the 5′-UTR. (**a**) Direct visualization of a bicistronic reporter activity with TBS in the 5′-UTR after co-transfection of 293T cells in a 35 mm dish with 1 μg pTBS/5Y-YIC DNA and 1 μg TRAP-expression DNA (TRAP) or 3 μg pUC19 DNA (no TRAP). Scale bar, 40 μm. (**b**) Dose- and TBS-dependent repression of YFP expression by TRAP. The 293T cells grown in 60 mm dishes were co-transfected with 2 μg of pTBS/5Y-YIC or control pYIC DNA along with the indicated amount of TRAP-expression DNA and were analyzed for YFP and CFP fluorescence, 24 h after transfection. Each bar represents mean YFP/CFP fluorescence for 30 randomly selected cells and its SD. (**c**) Western blot analysis of cytoplasmic extracts prepared from the pool of cells imaged in (b) with anti-His_6 antibody used to detect His_6-tagged TRAP, CFP and YFP, as indicated. (**d** and **e**) Position dependence of TRAP-mediated repression. To determine the effect of placing TBS downstream of the 5′-UTR, microscopic and western blot analyses were performed 24 h after transfection of 293T cells in a 60 mm dish with 2 μg of pTBS/iY-YIC, pTBS/3Y-YIC or pTBS/3C-YIC DNA, along with no (solid bar) or 6 μg (open bar) TRAP-expression DNA. (**f**) Coefficient of variation for samples plotted in (b) showing the value of normalizing YFP signal by CFP (compare yellow and brown bars within each group for '−TBS' and '+TBS, 0 μg TRAP') and a sharp rise in YFP/CFP coefficient of variation upon TRAP interaction with TBS in the 5′-UTR (compare brown bars of '+TBS, TRAP' with the brown bar of '+TBS, 0 μg TRAP'). +TBS and −TBS refer to pTBS/5Y-YIC and pYIC samples in (b), respectively.

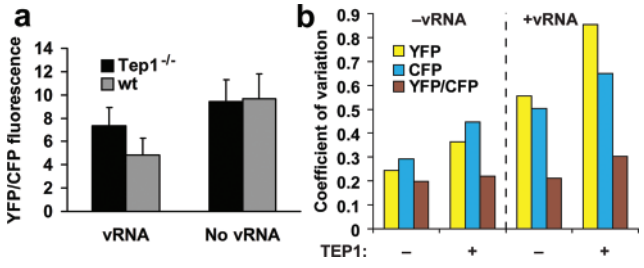

Figure 4. TEP1 interaction with vRNA as assessed by selective translational repression of a vRNA-containing bicistronic reporter transcript. (**a**) Relative YFP fluorescence was determined from YFP and CFP signals detected by fluorescence microscopy from wild-type *mTep1*$^{+/+}$ (wt) and its congenic *mTep1*-knockout (*mTep1*$^{-/-}$) cells transiently transfected with a bicistronic reporter gene containing vRNA in the 5′-UTR, pvRNA-YIC or a bicistronic reporter gene lacking vRNA, pYIC. Wilcoxon rank sum test shows statistically significant reduction of YFP/CFP fluorescence in the wild-type cells expressing TEP1 compared to the knockout for the vRNA-containing bicistronic reporter gene (*P*-value = 5.61×10^{-7}) but no significant difference for the vRNA-lacking bicistronic reporter gene (*P*-value = 0.76). Error bars are SDs for a sample size of 30. (**b**) Coefficient of variation for the fluorescence data in (a) showing an increase in the coefficient of variation for YFP/CFP fluorescence in the sample with potential for TEP1–vRNA interaction (compare brown bar of '+vRNA, +*mTep1*' with that of '+vRNA, −*mTep1*'). As the Wilcoxon rank sum test showed in (a), this increase is statistically significant.

Dynamic range for repressors

Although TRAP–TBS interaction showed that two orders of magnitude translational repression with the bicistronic reporter gene can be achieved, the TEP1–vRNA interaction showed the bicistronic translational repression assay to be highly sensitive. Wild-type *mTep1*$^{+/+}$ (wt) cells transfected with vRNA-containing bicistronic reporter gene, pvRNA-YIC (Figure 1b), showed a small but significant decrease in YFP/CFP fluorescence of ∼1.5-fold compared to *mTep1*$^{-/-}$ cells (4.84×1.46 versus 7.36 ± 1.55, Table 1 and Figure 4a; *P*-value = 5.61×10^{-7}), but no significant difference for vRNA-lacking bicistronic gene [9.68 ± 2.12 (*mTep1*$^{+/+}$) and 9.44 ± 1.86 (*mTep1*$^{-/-}$), Table 1 and Figure 4a; *P*-value = 0.76], indicating that TEP1–vRNA interaction selectively repressed cap-dependent translation in *mTep1*$^{+/+}$ cells. Analysis of YFP/CFP coefficient of variation also showed the expected increase in its value, consistent with selective translational repression by TEP1–vRNA interaction (Figure 4b). Thus, the bicistronic gene coupled to microscopic analysis is sensitive to small differential changes and can assess RNA–protein interaction causing selective decrease in cap-dependent translation over ∼1.5- to ∼180-fold range.

Detection of a different mode of translational regulation

As a final test for the reliability of this microscopy-based bicistronic translational repression assay, we examined the interaction of MS2-CP with its binding site, which has been shown to inhibit cap-dependent translation (17,18). Interestingly, although two MS2-binding sites, 2xMS2, at the 5′-UTR of a bicistronic gene significantly reduced YFP/CFP fluorescence 6-fold from ∼14.4 to ∼2.3 (Figure 5a, solid bars; *P*-value = 3.04×10^{-11}), to our surprise, expression of MS2-CP had no significant effect on YFP/CFP ratio [2.31 ± 0.67 (no MS2-CP), 2.53 ± 0.62 (MS2-CP); Figure 5a and Table 1; *P*-value = 0.20]. In contrast, analysis of individual

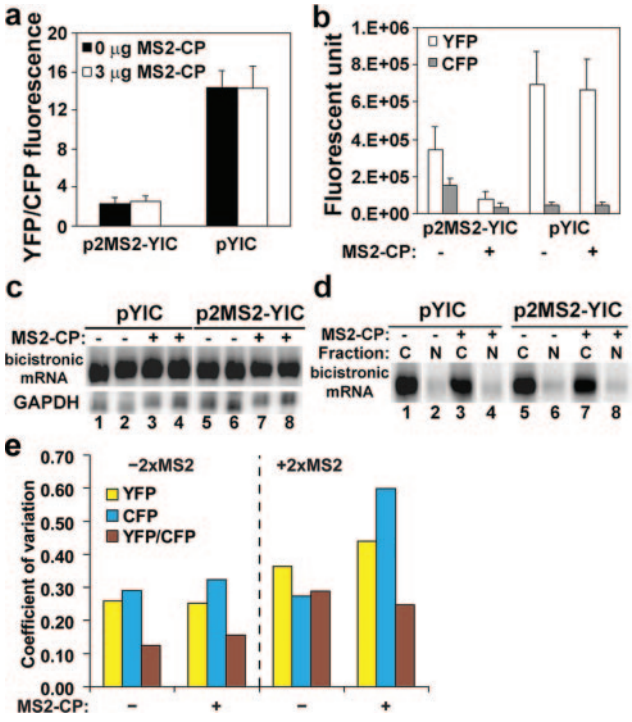

Figure 5. Different mode of translational repression by MS2-CP. (**a**) Effect of MS2-CP on relative YFP/CFP fluorescence. The 293T cells grown in 35 mm dishes were transfected with 1 μg of p2MS2-YIC or control pYIC DNA along with no or 3 μg MS2-CP expression DNA and analyzed for YFP/CFP fluorescence 24 h after transfection. MS2-CP had no significant effect on YFP/CFP fluorescence (*P*-value = 0.20 for 2xMS2-containing bicistronic gene; *P*-value = 0.97 for 2xMS2-lacking bicistronic gene). (**b**) Analysis of individual fluorescence. Mean of YFP and CFP fluorescence for a 10-pixel circle from cells analyzed in (a) are plotted as arbitrary fluorescence unit ($n = 30$). Error bar is SD. Note MS2-CP significantly decreased 2xMS2-containing bicistronic gene activity 4-fold (*P*-value = 4.10×10^{-11} for YFP fluorescence and *P*-value = 5.52×10^{-11} for CFP fluorescence) but had no significant effect on 2xMS2-lacking bicistronic gene activity (*P*-value = 0.48 for YFP fluorescence and *P*-value = 0.51 for CFP fluorescence). (**c**) Northern blot analysis of total RNA. Duplicate transfections performed at the same time as in (a) were analyzed for presence of bicistronic (upper panels) or GAPDH (lower panels) mRNAs using ^{32}P-labeled RNA probes. Images collected on PhosphorImager (Molecular Dynamics) are shown. (**d**) Effect of MS2-CP on nuclear/cytoplasmic partition of bicistronic mRNA. Northern blot analysis on duplicate samples fractionated for cytoplasm (odd) or nucleus (even) were analyzed for presence of bicistronic mRNA, as in (c). Ethidium bromide staining of gel fractionated RNAs revealed expected presence of precursor rRNA in the nuclear but not cytoplasmic fraction (data not shown). (**e**) Coefficient of variation for the fluorescence data in (a and b). Unlike the previous three RNA–protein interactions which led to an increase in the coefficient of variation for YFP/CFP fluorescence ratio, MS2-CP failed to cause an increase in this coefficient for the 2xMS2-containing bicistronic reporter gene (compare brown bar of '+2xMS2, −MS2-CP' with that of '+2xMS2, +MS2-CP'). The slight decrease observed is not statistically significant as the Wilcoxon rank sum test gave a *P*-value = 0.20. This failure to cause a rise in the coefficient of variation for YFP/CFP fluorescence ratio probably reflects a different mechanism of translational repression through the 5′-UTR, namely translational repression of the entire bicistronic reporter transcript with the 2xMS2 site in the presence of MS2-CP. +2xMS2 and −2xMS2 refer to p2MS2-YIC and pYIC samples in (a) and (b), respectively.

fluorescence (Figure 5b) showed MS2-CP to cause a 4-fold reduction in YFP and CFP fluorescence for the 2xMS2-containing bicistronic reporter mRNA [p2MS2-YIC; *P*-value = 4.10×10^{-11} (YFP) and 5.52×10^{-11} (CFP)] but no significant effect in the absence of its binding sites [pYIC;

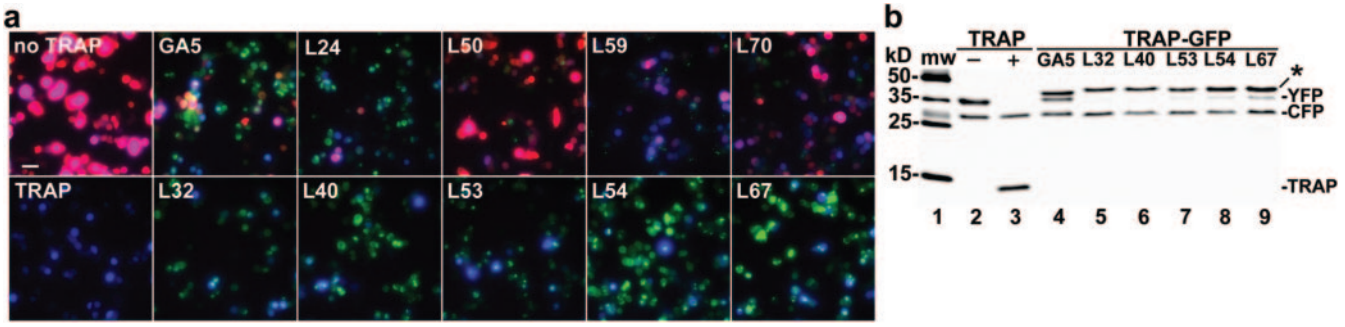

Figure 6. Screen for linkers that support RNA-binding activity of TRAP. (**a**) Visual analysis of DsRed2 (pseudocolored red), GFP (pseudocolored green) and CFP (pseudocolored blue) fluorescence in a single field of cells, following fluorescence microscopy and overlay of the three distinct signals. The 293T cells were transfected in 24-well plates with a modified pYIC/5Y-YIC bicistronic reporter gene alone in which the upstream YFP-encoding cistron was replaced with DsRed2 encoding sequences (upper left-hand panel) or co-transfected with expression DNA for TRAP (lower left-hand panel), TRAP–GFP fused through a GA5 linker (upper second panel from left) or TRAP–GFP fused through two different series of linkers with randomized sequences (panels designated with L and a number). Potential positive linkers are those with decreased DsRed2 fluorescence compared to GA5 panel as seen for the bottom panels starting with the second panel on the left. (**b**) Western blot analysis of potential positive linkers for TRAP–GFP. Ability of TRAP–GFP to selectively repress cap-dependent translation was analyzed using the YFP- and TBS-containing bicistronic reporter gene (pTBS/5Y-YIC). Note the relative level YFP to CFP is lower for the five potential linkers (lanes 5–9) from the visual screen [lower panels of (a)] than the GA5 linker (lane 4). Longer exposure shows that linker L40 (lane 6) appears to fully repress YFP translation, analogous to the level seen for TRAP (lane 3) (data not shown). Asterisk denotes location of TRAP–GFP.

P-value = 0.48 (YFP) and 0.51 (CFP)]. Northern blot analysis on total RNA extracted 24 h after transfection showed no change in steady-state level or intactness of the bicistronic mRNAs, thus MS2-CP did not affect mRNA synthesis, turnover or intactness (Figure 5c). RNA samples from nuclear and cytoplasmic fractions contained no noticeable difference in the relative abundance of the bicistronic message, indicating that the 2xMS2-containing message was not retained in the nucleus (Figure 5d). Together these results showed that MS2-CP interacted with the 2xMS2-containing bicistronic mRNA in a manner which led to a decrease in translation of both cistrons rather than selective translational repression of the upstream cistron; this effect on expression of the entire reporter transcript is not due to transfection efficiency, transcription, RNA turnover, or nuclear retention as shown in Figure 5c and d (in addition see Discussion).

Failure of MS2-CP interaction with 2xMS2 site in the 5′-UTR to cause selective translational repression is also reflected in the YFP/CFP coefficient of variation analysis, which no longer increased with this RNA–protein interaction but rather showed a non-statistically significant reduction (Figure 5e, *P*-value = 0.20), further highlighting YFP/CFP coefficient of variation as an indicator for selective translational repression. Thus, the bicistronic translational repression assay detects different modes of translational repression—selective repression of cap-dependent translation for three RNA-binding proteins and global repression of the entire bicistronic transcript affecting both cap- and IRES-dependent translation by MS2-CP.

Limited genetic screen for linkers that support RNA-binding activity of TRAP

A limited screen for linkers that support RNA-binding activity in TRAP–GFP fusion protein was conducted with a modified bicistronic reporter gene, substituting YFP with red fluorescent protein (DsRed2; Clontech) coding sequence in pTBS/5Y-YIC DNA (Figure 1b). Inserting a 26-bp linker with a 9–amino acid, random sequence or a 56-bp linker with a 19-amino acid, random sequence in frame with 5 glycine-alanine repeats (GA5 linker) used previously to fuse TRAP to GFP (EGFP; Clontech) generated a limited collection of random linkers. To avoid stop codons in one orientation, each triplet codon in the third position was a pyrimidine nucleotide.

The 293T cells transfected with the modified bicistronic gene are red-magenta without TRAP and blue upon co-transfection with non-GFP-labeled TRAP-expression DNA (Figure 6a, overlay of all three fluorescence: DsRed2-pseudocolored red, CFP-pseudocolored blue and GFP-pseudocolored green). For TRAP–GFP with GA5 linker, all three primary colors are observed in addition to other colors (yellow, cyan, magenta, white and so on) from mixing of the three primary colors. Using GA5 linker as reference, 105 independent random linkers were screened for improved RNA-binding ability as TRAP–GFP fusion protein, yielding 14 potential positive linkers (2/25 for the shorter linker and 12/80 for the longer linker). Lower panels (L32, L40, L53, L54 and L67) show 5 of the 14 potential positive linkers, while upper panels (L24, L50, L59 and L70) show linkers that were considered negative. Western blot analysis showed the 14 linkers to selectively repress cap-dependent translation to a greater extent than the GA5 linker (Figure 6b and data not shown), and in some cases (e.g. L40 linker) to a level comparable to the non-GFP-labeled TRAP (Figure 6b, compare lanes 6 and 3). Thus, a screen in mammalian cells based on translational repression to isolate RNA-binding proteins with desired characteristics is feasible.

DISCUSSION

Here, we describe a general method to directly assess RNA–protein interaction and translational repression in cultured mammalian cells, based on a well-documented phenomenon of translational repression by sequence-specific RNA–protein interaction at the 5′-UTR (7,10,11,13–22,43,44,56,57). This phenomenon has also been used in a proof-of-concept

experiment to screen for a RNA-binding activity in yeast cells (18). However, given typical translational repression in a reporter assay at about one order of magnitude (10,15–22,43–45), the proof-of-concept experiment required multiple rounds of cell sorting with a fluorescence-activated cell sorter on an initial pool of stable yeast transformants to isolate yeast with a particular RNA-binding activity (18). Based on the same biological phenomenon, we sought an alternative strategy that permits direct assessment of a specific RNA-binding activity and translational repression from a single pass examination of transiently transfected living mammalian cells, as normally encountered in a microscope field. Using a bicistronic reporter gene with independent sites for translational initiation of two spectrally distinct fluorescent proteins, we were able to assess RNA–protein interaction *in situ* through translational repression mediated by RNA–protein complexes at the 5′-UTR (Figure 1a). The second cistron with independent ribosome loading serves as an important internal control to permit qualitative and quantitative cell-by-cell assessment of translational repression affecting the first cistron.

Characterization of four distinct RNA–protein pairs by digital fluorescence microscopy showed ∼1.5- to ∼180-fold translational repression, establishing the sensitivity and dynamic range of the bicistronic translational repression assay in human and mouse cells (Table 1). The 5-fold translational repression for IRE–IRP interaction and 4-fold for 2xMS2–MS2-CP interaction are within the reported range of 1.5- to 15-fold for the former (10,16,18,44,45) and 3- to 20-fold for the latter (17,18) in eukaryotic cells. For vRNA interaction with TEP1 (50,60) and TBS interaction with *B.subtilis* TRAP (9), these interactions have not been analyzed previously for translational repression through the 5′-UTR in eukaryotic cells, and are shown here, to lead to weak (∼1.5-fold) and strong (∼180-fold) repression of translation, respectively (Figures 3 and 4). In the case of *B.subtilis* TRAP, its ability to repress the translation of a TBS-containing mRNA suggests availability of free L-tryptophan in the cytoplasm to serve as a ligand for TRAP, and consequently, to permit TRAP to bind RNA (26–31). Validity of the visualization results were confirmed through western blot analyses of the expressed reporter proteins (Figure 3b–e).

Although binding affinity is important for the formation of a specific RNA–protein complex, the magnitude of translational repression appears to be relatively insensitive to differences in binding affinities (18). For two RNA-binding proteins used in this study, binding affinities of 1.0–10 nM for IRE–IRP interaction and 0.02–0.1 nM for MS2-CP interaction with its wild-type-binding site have been reported previously [summarized in (18)]. However, TRAP with an intermediate binding affinity (24,29,31–34) showed the most potent repression, followed by IRE–IRP and then MS2-CP with 2xMS2 binding site (Table 1), illustrating a lack of strict correlation between binding affinity and magnitude of repression. Other factors that contribute to the magnitude of repression are location of the RNA–protein complex along the 5′-UTR (13–15,63), base-line translation of the binding site-containing reporter transcript, e.g. 2xMS2 binding site (Figure 5a, closed bars), availability and conformation of the binding site in the reporter transcript, and effectiveness of a specific RNA–protein complex to block recruitment or scanning of the 43S translational preinitiation complex (13–15,19).

B.subtilis TRAP–TBS interaction in the 5′-UTR shows a dose-dependent decrease in YFP expression with little effect on CFP, achieving over two orders of magnitude translational repression at the highest expression level tested in mammalian cells (Figure 3b and c and Table 1). This potent repression of translation by TRAP is especially noteworthy as typical translational repression is about one order of magnitude, seen for the three other binding proteins examined here (Figures 2, 4 and 5 and Table 1) and previously reported in other studies (10,15–17,19–22,43–45). Unlike the RNA-binding proteins which recognize a folded RNA secondary structure or a limited stretch of single-stranded RNA (20,23,60,64,65), *B.subtilis* TRAP interaction with its 55 nt consensus RNA sequence is unique in that TRAP binds to an extended stretch of single-stranded RNA; this single-stranded RNA is wrapped intimately around the perimeter of TRAP's toroidal surface (36–38). Potency of TRAP's translational repression suggests efficient recognition of its binding site in the 5′-UTR and effective interference with 5′ cap-dependent recruitment of the 43S translational preinitiation complex (12–14,22), or alternatively, effective inhibition of the recruited complex scanning for the AUG initiator codon (14,19). Further contributing to the large change in translational repression is the high degree of base-line translation exhibited by the TBS-containing reporter transcript (Figure 3b, 9 μg, compare open and closed bars), allowing for a greater range of translational repression by TRAP. With optimal placement of the consensus TRAP-binding site within the 5′-UTR, the degree of repression may exceed the ∼180-fold observed in the current study. However, once translation has initiated, TRAP fails to inhibit the progression of the translating ribosome, as placement of TRAP-binding site in the translated region or near the terminator codon did not alter the translation of the bicistronic reporter mRNA.

In general, the relatively low level of translational repression by specific RNA–protein interaction at the 5′-UTR in eukaryotic cells (10,15–22,43–45) has been considered disappointing (16), and translational repression by sequence-specific RNA-binding protein through the 5′-UTR has largely been ignored as a mechanism for regulating gene expression in mammalian cells. Indeed, additional layers of regulatory control often accompany translational repression by sequence-specific RNA-binding protein through the 5′-UTR to achieve greater magnitude of regulated gene expression (16,22). In one demonstrated case, iron regulation of IRP–IRE interaction at the 5′-UTR is used in conjunction with a metallothionein promoter to obtain >500-fold induction in mammalian cells with translational regulation contributing about one order of magnitude to the regulated expression system (44). Only recently has translational repression by sequence-specific RNA-binding protein through the 5′-UTR solely as a mode of regulating gene expression been explored to control gene expression in plants (66) and protozoan (67). With results shown here, it is clear that translational repression by sequence-specific RNA-binding protein through the 5′-UTR can be robust in mammalian cells, and that *B.subtilis* TRAP or other similar sequence-specific RNA-binding proteins that bind over an extended region of single-stranded

RNA may be good candidates for developing a translational repression-based regulated gene expression system.

Although TRAP, IRPs and TEP1 showed a similar mode of translational repression, MS2-CP appeared to repress translation by a different mechanism. The first three binding proteins displayed the hallmark for selective translational repression, i.e. a decrease in YFP/CFP fluorescence (Figures 2b, 3b and 4a) coupled with an increase in its coefficient of variation (Figures 2c, 3f and 4b), which was not seen with MS2-CP (Figure 5a and e, brown bars of the last two groups on the right). Instead, expression of MS2-CP decreased both YFP and CFP signals 4-fold (Figure 5b, two groups on the left). This decrease is not a consequence of MS2-CP titrating out a protein required for both cap- and IRES-dependent translation (41), as the decline is specific only for the 2xMS2-containing bicistronic reporter mRNA (Figure 5b, compare left and right halves). Furthermore, this effect on expression is not due to transfection efficiency, transcription, RNA turnover, or nuclear retention (see Results). Given the propensity of MS2-CP to self-assemble into an icosahedral structure (68,69) and its ability to encapsidate heterologous RNAs containing its binding site (61,62), the observed decline in both YFP and CFP signals is most likely due to sequestration of the 2xMS2-containing bicistronic reporter transcript by MS2-CP, leading to coordinate repression of translation. Such a mode of translational repression by wild-type MS2-CP would not be apparent with a monocistronic message (17,18).

Development of the microscopy-based assay allowed a limited screen to be conducted for linkers that preserved the RNA-binding activity of TRAP within the context of a fusion protein to GFP (Figure 6). From the screen, TRAP–GFP fusion proteins with RNA-binding activity comparable to TRAP alone or with compromised RNA-binding activity were identified. In the latter case, the underlying mechanism responsible for loss of translational repression by either shorter or longer linkers remains to be determined. Loss of RNA binding could be due to direct interaction between the linker and TRAP's RNA-binding surface, interference with the oligomerization of individual TRAP subunits by the linker or GFP, or altered conformation of the TRAP 11-mer complex affecting L-tryptophan or RNA binding. Although visual inspection sufficed in our limited screen to identify cells with potentially positive linkers, the ability to reduce the visual data to a set of numeric values (ratiometric, absolute and coefficient of variation) should facilitate large-scale screens in mammalian cells for a particular RNA–protein interaction with currently available automated cell-imaging platforms (70–72).

In summary, we describe a microscopy-based bicistronic translational repression assay to assess RNA–protein interaction and translational repression in transiently transfected living mammalian cells. Examination of four RNA-binding proteins reveals a range of translational repression from ~1.5- to >180-fold, indicating that translational repression by sequence-specific RNA-binding protein through the 5′-UTR can be robust. As *B.subtilis* TRAP shows most potent translation repression, this class of RNA-binding proteins which recognize an extended single-stranded region may be good candidates in the design of a regulated mammalian gene expression system based on translational repression by a sequence-specific RNA-binding protein interacting with its binding site in the 5′-UTR. The assay showed two distinct modes of translational repression by sequence-specific RNA–protein interaction at the 5′-UTR, leading to either selective or coordinate repression of translation, the latter observed for a binding protein known to undergo self-assembly to form virion capsid structures. Finally, the ability to directly assess RNA–protein interaction from examination of 30 transiently transfected cells permitted a screen to identify linkers which support RNA-binding activity comparable to wild-type level within the context of a fusion protein, demonstrating the feasibility of conducting a screen in mammalian cells for a specific RNA-binding activity based on translational repression through the 5′-UTR.

ACKNOWLEDGEMENTS

We thank Stephanie M. Betancourt and Jean Oak for excellent technical assistance, Valerie A. Kickhoefer, Lea Harrington and Leonard H. Rome for generously supplying mouse vRNA DNA and knockout and wild-type TEP1 cell lines, Douglas L. Black for MS2-CP DNA, Valerie A. Kickhoefer, Leonard H. Rome, Asim Dasgupta and Robert Simons for helpful advice, discussion and critical reading of our manuscript. This work is in part supported by a grant from the UCLA Frontiers of Science Program. Funding to pay the Open Access publication charges for this article was provided by UCLA.

Conflict of interest statement. None declared.

REFERENCES

1. Celander,D.W. and Abelson,J. (2000) *RNA–Ligand Interactions*. Academic Press, San Diego, CA.
2. Maquat,L.E. (2002) RNA–protein interactions: insight into gene function. *Methods*, **26**, 93–94.
3. Rackham,O. and Brown,C.M. (2004) Visualization of RNA–protein interactions in living cells: FMRP and IMP1 interact on mRNAs. *EMBO J.*, **23**, 3346–3355.
4. Ule,J., Jensen,K., Mele,A. and Darnell,R.B. (2005) CLIP: a method for identifying protein–RNA interaction sites in living cells. *Methods*, **37**, 376–386.
5. Zielinski,J., Kilk,K., Peritz,T., Kannanayakal,T., Miyashiro,K.Y., Eiriksdottir,E., Jochems,J., Langel,U. and Eberwine,J. (2006) *In vivo* identification of ribonucleoprotein–RNA interactions. *Proc. Natl Acad. Sci. USA*, **103**, 1557–1562.
6. Hook,B., Bernstein,D., Zhang,B. and Wickens,M. (2005) RNA–protein interactions in the yeast three-hybrid system: affinity, sensitivity, and enhanced library screening. *RNA*, **11**, 227–233.
7. Wilkie,G.S., Dickson,K.S. and Gray,N.K. (2003) Regulation of mRNA translation by 5′- and 3′-UTR-binding factors. *Trends Biochem. Sci.*, **28**, 182–188.
8. Romby,P. and Springer,M. (2003) Bacterial translational control at atomic resolution. *Trends Genet.*, **19**, 155–161.
9. Gollnick,P., Babitzke,P., Antson,A. and Yanofsky,C. (2005) Complexity in regulation of tryptophan biosynthesis in *Bacillus subtilis*. *Annu. Rev. Genet.*, **39**, 47–68.
10. Hentze,M.W., Caughman,S.W., Rouault,T.A., Barriocanal,J.G., Dancis,A., Harford,J.B. and Klausner,R.D. (1987) Identification of the iron-responsive element for the translational regulation of human ferritin mRNA. *Science*, **238**, 1570–1573.
11. Rouault,T.A., Hentze,M.W., Caughman,S.W., Harford,J.B. and Klausner,R.D. (1988) Binding of a cytosolic protein to the iron-responsive element of human ferritin messenger RNA. *Science*, **241**, 1207–1210.

12. Gray,N.K. and Hentze,M.W. (1994) Iron regulatory protein prevents binding of the 43S translation pre-initiation complex to ferritin and eALAS mRNAs. *EMBO J.*, **13**, 3882–3891.
13. Muckenthaler,M., Gray,N.K. and Hentze,M.W. (1998) IRP-1 binding to ferritin mRNA prevents the recruitment of the small ribosomal subunit by the cap-binding complex eIF4F. *Mol. Cell*, **2**, 383–388.
14. Paraskeva,E., Gray,N.K., Schlager,B., Wehr,K. and Hentze,M.W. (1999) Ribosomal pausing and scanning arrest as mechanisms of translational regulation from cap-distal iron-responsive elements. *Mol. Cell. Biol.*, **19**, 807–816.
15. Goossen,B. and Hentze,M.W. (1992) Position is the critical determinant for function of iron-responsive elements as translational regulators. *Mol. Cell. Biol.*, **12**, 1959–1966.
16. Coulson,R.M. and Cleveland,D.W. (1993) Ferritin synthesis is controlled by iron-dependent translational derepression and by changes in synthesis/transport of nuclear ferritin RNAs. *Proc. Natl Acad. Sci. USA*, **90**, 7613–7617.
17. Stripecke,R., Oliveira,C.C., McCarthy,J.E. and Hentze,M.W. (1994) Proteins binding to 5′ untranslated region sites: a general mechanism for translational regulation of mRNAs in human and yeast cells. *Mol. Cell. Biol.*, **14**, 5898–5909.
18. Paraskeva,E., Atzberger,A. and Hentze,M.W. (1998) A translational repression assay procedure (TRAP) for RNA–protein interactions *in vivo*. *Proc. Natl Acad. Sci. USA*, **95**, 951–956.
19. Bag,J. (2001) Feedback inhibition of poly(A)-binding protein mRNA translation. A possible mechanism of translation arrest by stalled 40 S ribosomal subunits. *J. Biol. Chem.*, **276**, 47352–47360.
20. Nielsen,J., Christiansen,J., Lykke-Andersen,J., Johnsen,A.H., Wewer,U.M. and Nielsen,F.C. (1999) A family of insulin-like growth factor II mRNA-binding proteins represses translation in late development. *Mol. Cell. Biol.*, **19**, 1262–1270.
21. Melo,E.O., de Melo Neto,O.P. and Martins de Sa,C. (2003) Adenosine-rich elements present in the 5′-untranslated region of PABP mRNA can selectively reduce the abundance and translation of CAT mRNAs *in vivo*. *FEBS Lett.*, **546**, 329–334.
22. Beckmann,K., Grskovic,M., Gebauer,F. and Hentze,M.W. (2005) A dual inhibitory mechanism restricts *msl-2* mRNA translation for dosage compensation in *Drosophila*. *Cell*, **122**, 529–540.
23. Antson,A.A. (2000) Single-stranded-RNA binding proteins. *Curr. Opin. Struct. Biol.*, **10**, 87–94.
24. Antson,A.A., Otridge,J., Brzozowski,A.M., Dodson,E.J., Dodson,G.G., Wilson,K.S., Smith,T.M., Yang,M., Kurecki,T. and Gollnick,P. (1995) The structure of *trp* RNA-binding attenuation protein. *Nature*, **374**, 693–700.
25. Antson,A.A., Brzozowski,A.M., Dodson,E.J., Dauter,Z., Wilson,K.S., Kurecki,T., Otridge,J. and Gollnick,P. (1994) 11-Fold symmetry of the *trp* RNA-binding attenuation protein (TRAP) from *Bacillus subtilis* determined by X-ray analysis. *J. Mol. Biol.*, **244**, 1–5.
26. Babitzke,P. and Yanofsky,C. (1993) Reconstitution of *Bacillus subtilis* trp attenuation *in vitro* with TRAP, the *trp* RNA-binding attenuation protein. *Proc. Natl Acad. Sci. USA*, **90**, 133–137.
27. Babitzke,P. and Yanofsky,C. (1995) Structural features of L-tryptophan required for activation of TRAP, the *trp* RNA-binding attenuation protein of *Bacillus subtilis*. *J. Biol. Chem.*, **270**, 12452–12456.
28. Babitzke,P., Yealy,J. and Campanelli,D. (1996) Interaction of the *trp* RNA-Binding attenuation protein (TRAP) of *Bacillus subtilis* with RNA: effects of the number of GAG repeats, the nucleotides separating adjacent repeats, and RNA secondary structure. *J. Bacteriol.*, **178**, 5159–5163.
29. Babitzke,P., Stults,J.T., Shire,S.J. and Yanofsky,C. (1994) TRAP, the *trp* RNA-binding attenuation protein of *Bacillus subtilis*, is a multisubunit complex that appears to recognize G/UAG repeats in the *trpEDCFBA* and *trpG* transcripts. *J. Biol. Chem.*, **269**, 16597–16604.
30. Otridge,J. and Gollnick,P. (1993) MtrB from *Bacillus subtilis* binds specifically to *trp* leader RNA in a tryptophan-dependent manner. *Proc. Natl Acad. Sci. USA*, **90**, 128–132.
31. Baumann,C., Xirasagar,S. and Gollnick,P. (1997) The *trp* RNA-binding attenuation protein (TRAP) from *Bacillus subtilis* binds to unstacked *trp* leader RNA. *J. Biol. Chem.*, **272**, 19863–19869.
32. Yang,M., Chen,X., Militello,K., Hoffman,R., Fernandez,B., Baumann,C. and Gollnick,P. (1997) Alanine-scanning mutagenesis of *Bacillus subtilis* trp RNA-binding attenuation protein (TRAP) reveals residues involved in tryptophan binding and RNA binding. *J. Mol. Biol.*, **270**, 696–710.
33. Baumann,C., Otridge,J. and Gollnick,P. (1996) Kinetic and thermodynamic analysis of the interaction between TRAP (*trp* RNA-binding attenuation protein) of *Bacillus subtilis* and *trp* leader RNA. *J. Biol. Chem.*, **271**, 12269–12274.
34. Elliott,M.B., Gottlieb,P.A. and Gollnick,P. (1999) Probing the TRAP–RNA interaction with nucleoside analogs. *RNA*, **5**, 1277–1289.
35. Chen,X., Antson,A.A., Yang,M., Li,P., Baumann,C., Dodson,E.J., Dodson,G.G. and Gollnick,P. (1999) Regulatory features of the *trp* operon and the crystal structure of the *trp* RNA-binding attenuation protein from *Bacillus stearothermophilus*. *J. Mol. Biol.*, **289**, 1003–1016.
36. Antson,A.A., Dodson,E.J., Dodson,G., Greaves,R.B., Chen,X. and Gollnick,P. (1999) Structure of the *trp* RNA-binding attenuation protein, TRAP, bound to RNA. *Nature*, **401**, 235–242.
37. Hopcroft,N.H., Wendt,A.L., Gollnick,P. and Antson,A.A. (2002) Specificity of TRAP–RNA interactions: crystal structures of two complexes with different RNA sequences. *Acta Crystallogr. D Biol. Crystallogr.*, **58**, 615–621.
38. Hopcroft,N.H., Manfredo,A., Wendt,A.L., Brzozowski,A.M., Gollnick,P. and Antson,A.A. (2004) The interaction of RNA with TRAP: the role of triplet repeats and separating spacer nucleotides. *J. Mol. Biol.*, **338**, 43–53.
39. Xirasagar,S., Elliott,M.B., Bartolini,W., Gollnick,P. and Gottlieb,P.A. (1998) RNA structure inhibits the TRAP (*trp* RNA-binding attenuation protein)–RNA interaction. *J. Biol. Chem.*, **273**, 27146–27153.
40. Yakhnin,H., Zhang,H., Yakhnin,A.V. and Babitzke,P. (2004) The *trp* RNA-binding attenuation protein of *Bacillus subtilis* regulates translation of the tryptophan transport gene *trpP* (*yhaG*) by blocking ribosome binding. *J. Bacteriol.*, **186**, 278–286.
41. Pestova,T.V., Kolupaeva,V.G., Lomakin,I.B., Pilipenko,E.V., Shatsky,I.N., Agol,V.I. and Hellen,C.U. (2001) Molecular mechanisms of translation initiation in eukaryotes. *Proc. Natl Acad. Sci. USA*, **98**, 7029–7036.
42. Shaner,N.C., Steinbach,P.A. and Tsien,R.Y. (2005) A guide to choosing fluorescent proteins. *Nature Methods*, **2**, 905–909.
43. Miller,S.J., Suthiphongchai,T., Zambetti,G.P. and Ewen,M.E. (2000) p53 binds selectively to the 5′ untranslated region of *cdk4*, an RNA element necessary and sufficient for transforming growth factor beta- and p53-mediated translational inhibition of cdk4. *Mol. Cell. Biol.*, **20**, 8420–8431.
44. Daniels-McQueen,S., Goessling,L.S. and Thach,R.E. (1992) Inducible expression bovine papillomavirus shuttle vectors containing ferritin translational regulatory elements. *Gene*, **122**, 271–279.
45. Henderson,R.J., Patton,S.M. and Connor,J.R. (2005) Development of a fluorescent reporter to assess iron regulatory protein activity in living cells. *Biochim. Biophys. Acta*, **1743**, 162–168.
46. Jarvik,J.W. and Telmer,C.A. (1998) Epitope tagging. *Annu. Rev. Genet.*, **32**, 601–618.
47. Borman,A.M., Le Mercier,P., Girard,M. and Kean,K.M. (1997) Comparison of picornaviral IRES-driven internal initiation of translation in cultured cells of different origins. *Nucleic Acids Res.*, **25**, 925–932.
48. SenGupta,D.J., Zhang,B., Kraemer,B., Pochart,P., Fields,S. and Wickens,M. (1996) A three-hybrid system to detect RNA–protein interactions *in vivo*. *Proc. Natl Acad. Sci. USA*, **93**, 8496–8501.
49. Bardwell,V.J. and Wickens,M. (1990) Purification of RNA and RNA–protein complexes by an R17 coat protein affinity method. *Nucleic Acids Res.*, **18**, 6587–6594.
50. Kickhoefer,V.A., Liu,Y., Kong,L.B., Snow,B.E., Stewart,P.L., Harrington,L. and Rome,L.H. (2001) The Telomerase/vault-associated protein TEP1 is required for vault RNA stability and its association with the vault particle. *J. Cell Biol.*, **152**, 157–164.
51. Min Jou,W., Haegeman,G., Ysebaert,M. and Fiers,W. (1972) Nucleotide sequence of the gene coding for the bacteriophage MS2 coat protein. *Nature*, **237**, 82–88.
52. Pear,W.S., Nolan,G.P., Scott,M.L. and Baltimore,D. (1993) Production of high-titer helper-free retroviruses by transient transfection. *Proc. Natl Acad. Sci. USA*, **90**, 8392–8396.
53. Chen,C. and Okayama,H. (1987) High-efficiency transformation of mammalian cells by plasmid DNA. *Mol. Cell. Biol.*, **7**, 2745–2752.
54. Walpole,R.E., Myers,R.H. and Myers,S.L. (1998) *Probability and Statistics For Engineers and Scientists, 6th edn*. Prentice Hall, Upper Saddle River, NJ.

55. Sambrook,J. and Russell,D.W. (2001) *Molecular Cloning: A Laboratory Manual. 3rd edn*. Cold Spring Harbor Laboratory Press, Cold Spring Harbor, NY.
56. Gu,W. and Hecht,N.B. (1996) Translation of a testis-specific Cu/Zn superoxide dismutase (SOD-1) mRNA is regulated by a 65-kilodalton protein which binds to its 5′ untranslated region. *Mol. Cell. Biol*., **16**, 4535–4543.
57. Meyuhas,O. (2000) Synthesis of the translational apparatus is regulated at the translational level. *Eur. J. Biochem*., **267**, 6321–6330.
58. De Gregorio,E., Preiss,T. and Hentze,M.W. (1999) Translation driven by an eIF4G core domain *in vivo*. *EMBO J*., **18**, 4865–4874.
59. Chen,C.Y. and Sarnow,P. (1995) Initiation of protein synthesis by the eukaryotic translational apparatus on circular RNAs. *Science*, **268**, 415–417.
60. Poderycki,M.J., Rome,L.H., Harrington,L. and Kickhoefer,V.A. (2005) The p80 homology region of TEP1 is sufficient for its association with the telomerase and vault RNAs, and the vault particle. *Nucleic Acids Res*., **33**, 893–902.
61. Pickett,G.G. and Peabody,D.S. (1993) Encapsidation of heterologous RNAs by bacteriophage MS2 coat protein. *Nucleic Acids Res*., **21**, 4621–4626.
62. Beckett,D., Wu,H.N. and Uhlenbeck,O.C. (1988) Roles of operator and non-operator RNA sequences in bacteriophage R17 capsid assembly. *J. Mol. Biol*., **204**, 939–947.
63. Stripecke,R. and Hentze,M.W. (1992) Bacteriophage and spliceosomal proteins function as position-dependent *cis*/*trans* repressors of mRNA translation *in vitro*. *Nucleic Acids Res*., **20**, 5555–5564.
64. Chen,Y. and Varani,G. (2005) Protein families and RNA recognition. *FEBS J*., **272**, 2088–2097.
65. De Guzman,R.N., Turner,R.B. and Summers,M.F. (1998) Protein–RNA recognition. *Biopolymers*, **48**, 181–195.
66. Cerny,R.E., Qi,Y., Aydt,C.M., Huang,S., Listello,J.J., Fabbri,B.J., Conner,T.W., Crossland,L. and Huang,J. (2003) RNA-binding protein-mediated translational repression of transgene expression in plants. *Plant Mol. Biol*., **52**, 357–369.
67. Shi,H., Djikeng,A., Chamond,N., Ngo,H., Tschudi,C. and Ullu,E. (2005) Repression of gene expression by the coliphage MS2 coat protein in *Trypanosoma brucei*. *Mol. Biochem. Parasitol*., **144**, 119–122.
68. Beckett,D. and Uhlenbeck,O.C. (1988) Ribonucleoprotein complexes of R17 coat protein and a translational operator analog. *J. Mol. Biol*., **204**, 927–938.
69. Valegard,K., Murray,J.B., Stonehouse,N.J., van den Worm,S., Stockley,P.G. and Liljas,L. (1997) The three-dimensional structures of two complexes between recombinant MS2 capsids and RNA operator fragments reveal sequence-specific protein–RNA interactions. *J. Mol. Biol*., **270**, 724–738.
70. Lang,P., Yeow,K., Nichols,A. and Scheer,A. (2006) Cellular imaging in drug discovery. *Nature Rev. Drug Discov*., **5**, 343–356.
71. Smellie,A., Wilson,C.J. and Ng,S.C. (2006) Visualization and interpretation of high content screening data. *J. Chem. Inf. Model*, **46**, 201–207.
72. Abraham,V.C., Taylor,D.L. and Haskins,J.R. (2004) High content screening applied to large-scale cell biology. *Trends Biotechnol*., **22**, 15–22.